Available online at www.sciencedirect.com
ScienceDirect
International Journal of Heat and Mass Transfer 51 (2008) 3571–3581
International Journal of HEAT and MASS TRANSFER
www.elsevier.com/locate/ijhmt

Inverse estimation of heat flux and temperature on nozzle throat-insert inner contour

Tsung-Chien Chen [a,*], Chiun-Chien Liu [b]

[a] Department of Power Vehicle and Systems Engineering, Chung Cheng Institute of Technology, National Defense University, Ta-Hsi, Tao-Yuan 33509, Taiwan, ROC
[b] Chung Shan Institute of Science and Technology, Lung-Tan, Tao-Yuan 32526, Taiwan, ROC

Received 21 February 2007; received in revised form 15 October 2007
Available online 28 January 2008

Abstract

During the missile flight, the jet flow with high temperature comes from the heat flux of propellant burning. An enormous heat flux from the nozzle throat-insert inner contour conducted into the nozzle shell will degrade the material strength of nozzle shell and reduce the nozzle thrust efficiency. In this paper, an on-line inverse method based on the input estimation method combined with the finite-element scheme is proposed to inversely estimate the unknown heat flux on the nozzle throat-insert inner contour and the inner wall temperature by applying the temperature measurements of the nozzle throat-insert. The finite-element scheme can easily define the irregularly shaped boundary. The superior capability of the proposed method is demonstrated in two major time-varying estimation cases. The computational results show that the proposed method has good estimation performance and highly facilitates the practical implementation. An effective analytical method can be offered to increase the operation reliability and thermal-resistance layer design in the solid rocket motor.

Keywords: Heat flux; Input estimation method; Finite-element scheme

1. Introduction

The nozzle plays an important role in the solid rocket motor (SRM). The high temperature jet energy from the combustor produced by expansion and acceleration is transferred into the motor thrust and makes the missile flight possible. During the motor operation process, the nozzle must endure the impact of jet flow with high temperature and pressure. Under this situation, the nozzle design will obviously affect the motor performance. The high temperature from the inner contour of the nozzle conducted into its shell will increase the erosion of nozzle throat-insert, enlarge the throat radius which makes thrust descend, decrease the material strength of the nozzle shell, and reduce the nozzle thrust efficiency [1,2]. It will influence the performance of the missile. In order to meet the requirements in resisting the nozzle shell temperature and the jet flow, the throat-insert materials need to be inserted in the nozzle inner counter to form protection. There are three major materials required, which are the throat-insert, thermal liner and insulator materials. The nozzle throat endures serious impact from high temperature and the strongest heat flux in the throat-insert, so that the throat-insert materials will directly affect the nozzle efficiency and reliability [3]. Therefore, the heat conduction problem design in the nozzle and the method to choose moderate throat-insert materials is very important, since we are well informed of the fact that the high temperature can be produced by heat flux.

The unknown heat source or heat flux estimation utilizing a measured temperature inside a heat-conducting solid is called the inverse heat conduction problem (IHCP). It is necessary to calculate the transient surface heat flux and

* Corresponding author.
E-mail address: c2271003@ms61.hinet.net (T.-C. Chen).

0017-9310/$ - see front matter © 2007 Elsevier Ltd. All rights reserved.
doi:10.1016/j.ijheatmasstransfer.2007.10.029

Nomenclature

B	sensitivity matrix
$[C]$	capacitance matrix
C_p	specific heat
$[D]$	matrix of the conductivity values
E	elements number
$\{ff\}$	coefficient matrix
$\{F\}$	thermal load vector
$[G]$	coefficient matrix
H	measurement matrix
h	convection heat transfer coefficient
k	time (discretized)
K	Kalman gain
K_b	steady-state correction gain
K_{rr}, K_Z	thermal conductivity
L	length of z direction
M	sensitivity matrix
$[M]$	global conductance matrix
N	total number of spatial nodes
$[N]$	shape function matrix
P	filter's error covariance matrix
$q(t)$	continuous-time unknown heat flux input
$q(k)$	discrete-time unknown heat flux input
P_b	error covariance matrix
Q	process noise variance
r	axial direction
R	measurement noise variance
R_i	inner radial
R_o	outer radial
$s(k)$	innovation covariance
t	time
T	temperature
$\{T\}$	temperature vector
Δt	sampling time interval
v	measurement noise vector
X	state vector
z	axial direction
Z	observation vector
α	thermal diffusivity
γ	forgetting factor
Γ	input matrix
δ	Dirac delta function
ρ	density
Λ	coefficient matrix
Φ	state transition matrix
Ψ	coefficient matrix
Ω	coefficient matrix
Θ	coefficient matrix
σ	standard deviation of the measurement noise
ω	process noise vector

Subscripts

1, 2	sensor measurement location
s	body surface

Superscripts

$\bar{}$	estimated by filter
$\hat{}$	estimated
T	transpose of matrix
e	element

temperature distribution from the temperature measurements at some location inside or outside the body. For example, when evaluating new heat-shield materials, static firing test of rocket nozzles, and developing transient calorimeters, it is necessary to calculate the transient surface heat flux and temperature distribution from the temperature history measured at some location inside or outside the body. In the indirect approach, the thermocouples are embedded inside the body rather than on the surface where the boundary temperature is extremely high. By applying these temperature measurements to the inverse heat conduction methods, the unknown surface heat flux can be estimated. There are various theories about the IHCP, and the development of the solutions has already been in progress constantly. Those solutions can be assorted into two, major categories in terms of the data processing. One is the off-line estimation [4–8], and the other is the on-line estimation [9–14]. The off-line estimation processes the data in the batch form. The problem with the batch form is the computational inefficiency. To resolve the inefficiency issue of the batch form approach, Tuan et al. [9] in 1996 successfully developed an input estimation algorithm, which can on-line estimate an unknown input, such as the heat flux, heat sources, etc., as shown in the articles presented by Tuan et al. [9,10] and Ji et al. [11,12].

In this paper, the on-line estimation, which combines the input estimation method with the finite-element scheme, is adopted to solve the unknown heat flux problem and the 2D hollow cylinder nozzle IHCP. The discrete finite-element concept has been applied to the inverse heat conduction problems [15–19]. The irregularly shaped boundaries can be approximated using the elements with straight sides or matched using the elements with curved boundaries. The input estimation method uses the Kalman filter to generate the residual innovation sequence. A recursive least square algorithm is derived to compute the value of the heat flux by using this residual sequence [20]. The proposed method for the 2D hollow cylinder nozzle IHCP is also used to study the modeling and measurement error effects. The triangle waveform and Generalized bell curve function are utilized in the heat flux simulation cases. The results demonstrate good performance and precision in tracking the unknown boundary heat flux of a thermal system.

2. Problem formulation

We assume axis-symmetric transient heat conduction in hollow cylinder, where r, θ, z, are the radial, circumferential, and axial axes, respectively [21]. The nozzle insert-throat material is a non-homogeneous irregular shape heat conduction body. The governing equation is simplified in two-dimensional, $R_i \leqslant r \leqslant R_o$, $0 \leqslant z \leqslant L$. The initial temperature is $T(r,z,0) = 0$. For time $t > 0$ the boundaries at $z = 0$, $z = L$ and outer surface $r = R_o$ are kept insulated. The simulated measured temperature $Z(R_o, t)$ is located in the nozzle insert-throat material outer wall $m(r,z)$.To demonstrate the finite-element method application to temperature distribution determination with a conducting body, Fig. 1 shows the geometry and discrete models.

The following restrictions apply here:

(1) The temperature distribution is axis-symmetrical.
(2) The densities, specific heats, and thermal conductivities of the inner wall of nozzle are all constants.
(3) Phase change in the material is not considered to have an effect on the heat transfer process.
(4) The outer wall of nozzle insert-throat material is insulated boundary.

The mathematical formulation of the two-dimensional, transient, heat conduction problem can be generalized as

$$K_{rr}\frac{\partial^2 T}{\partial r^2} + \frac{K_{rr}}{r}\frac{\partial T}{\partial r} + K_{zz}\frac{\partial^2 T}{\partial z^2} = \rho C_p \frac{\partial T}{\partial t} \quad R_i \leqslant r \leqslant R_o,\ 0 \leqslant z \leqslant L,\ t > 0 \tag{1}$$

$$T(r,z,0) = T_0 = 0 \quad R_i \leqslant r \leqslant R_o,\ 0 \leqslant z \leqslant L,\ t = 0 \tag{2}$$

$$-K_{rr}\frac{\partial T}{\partial r} = q(z,t) \quad r = R_i,\ 0 \leqslant z \leqslant L \tag{3}$$

$$-K_{rr}\frac{\partial T}{\partial r} = 0 \quad r = R_o,\ 0 \leqslant z \leqslant L \tag{4}$$

$$\frac{\partial T}{\partial z} = 0 \quad R_i \leqslant r \leqslant R_o,\ z = 0 \tag{5}$$

$$\frac{\partial T}{\partial z} = 0 \quad R_i \leqslant r \leqslant R_o,\ z = L \tag{6}$$

$$Z_m(t) = T(R_o, z, t) + v(t) \tag{7}$$

where T_0 is the uniform initial temperature, $q(z,t)$ is the unknown heat flux inputs to be estimated. T is the temperature and t represent the time. There is a non-uniform distribution at the z axial and $Z_m(t)$ are the noise-corrupted temperature measurements. $v(t)$ is the measurement noise assumed with zero mean and white Gaussian noise.

The calculus of variations provides an alternative method for formulating the governing Eq. (1) and boundary conditions Eqs. (3)–(6). Variational calculus states that the minimization of the functional J [22]

$$J = \frac{1}{2}\iiint_V \left[rK_{rr}\left(\frac{\partial T}{\partial r}\right)^2 + rK_{zz}\left(\frac{\partial T}{\partial z}\right)^2 + 2r\rho C_p \frac{\partial T}{\partial t} T \right] \mathrm{d}V + \int_s [qT]\,\mathrm{d}S \tag{8}$$

$$J = \sum_{e=1}^{E} \int_{V^e} \frac{1}{2}\{T\}^{\mathrm{T}}\{B^e\}^{\mathrm{T}}[D^e]\{B^e\}\{T\}\,\mathrm{d}V$$

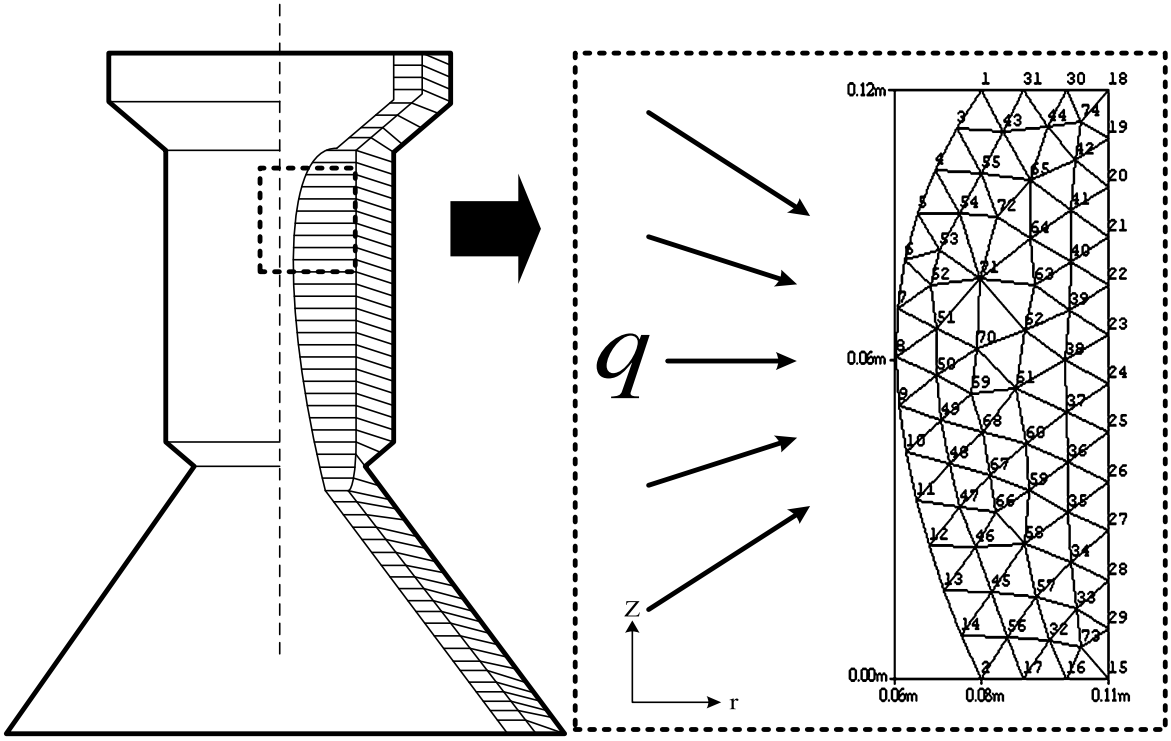

Fig. 1. Geometry and discrete models.

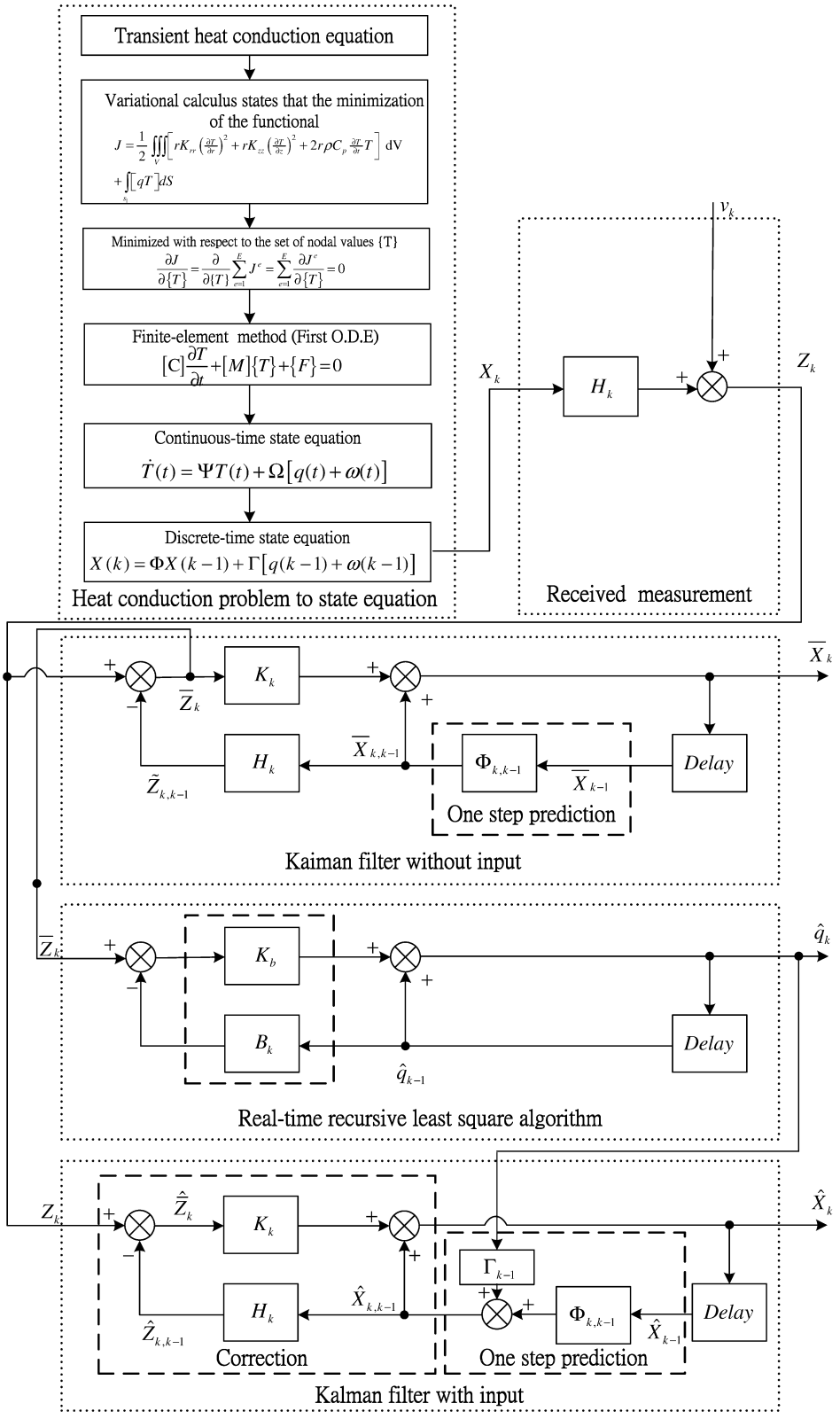

Fig. 2. A flow chart of the input estimation algorithm.

$$+\int_{V^e} r\rho C_p[N^e]\{T\}[N^e]\frac{\partial\{T\}}{\partial t}\,\mathrm{d}V + \int_{S^e} q[N^e]\{T\}\,\mathrm{d}S \tag{9}$$

Eq. (9) must be minimized with respect to the set of nodal temperature values $\{T\}$

$$\frac{\partial J}{\partial\{T\}} = \frac{\partial}{\partial\{T\}}\sum_{e=1}^{E} J^e = \sum_{e=1}^{E}\frac{\partial J^e}{\partial\{T\}} = 0 \tag{10}$$

When the minimization process is complete, the following system of equations results [23].

$$[C]\frac{\partial\{T\}}{\partial t}+[M]\{T\}+\{F\}=0 \tag{11}$$

Eq. (11) is the first-order linear differential equation of the system. The $[C]$ matrix is the global capacitance matrix, $[M]$ is the global conductance matrix, $\{F\}$ is the thermal load vector. The element contributions to $[C]$, $[M]$, $\{F\}$ are summed in the usual manner

$$[C]=\sum_{e=1}^{E}[C^e]=\sum_{e=1}^{E}\int_V r\rho C_p[N]^{\mathrm{T}}[N]\,\mathrm{d}V \tag{12}$$

$$[M]=\sum_{e=1}^{E}[M^e]=\sum_{e=1}^{E}\int_V [B]^{\mathrm{T}}[D][B]\,\mathrm{d}V \tag{13}$$

$$\{F\}=\sum_{e=1}^{E}\{f^e\}=\sum_{e=1}^{E}\int_{S_1} q[N]^{\mathrm{T}}\,\mathrm{d}S=[ff]\{q\} \tag{14}$$

where $[N]$ is the shape function matrix, $[B]$ is obtained by differentiating $[N]$ with respect to $r$and z, $[D]$ matrix consists of the conductivity values. $[ff]$ and $[G]$ are the coefficient matrix. q is the unknown heat flux input at the inner wall $r=R_{\mathrm{i}}$. All of the integrals in Eqs. (12)–(14) were evaluated over a single element. The element contributions are summed in the usual manner. Therefore, from Eq. (11) and to account for process noise inputs [24], the continuous-time state equation can be written as

$$\begin{aligned}\dot{T}(t)&=\Psi T(t)+\Omega[q(t)+\omega(t)]\\ \Psi&=(-1)[C]^{-1}[M]\\ \Omega&=(-1)[C]^{-1}[ff]\end{aligned} \tag{15}$$

where the state vector $T(t)$ is $N\times 1$. N is the total number of nodes. $\Psi$and Ω are both the coefficient matrices. $\omega(t)$ is the continuous-time processing error vector, which is assumed as the Gaussian white noise. The error exists in the formulation of the filter mathematical model due to the lack of understanding in the physical systems. $q(t)$ is the continuous-time unknown heat flux input.

Assume the state variable X represents the temperature, $q(k-1)$ is the discrete-time unknown heat flux input

$$\begin{aligned}X&=[\,T_1\quad T_2\quad T_3\quad\ldots\quad T_{N-1}\quad T_N\,]^{\mathrm{T}}\\ X(k)&=\Phi X(k-1)+\Gamma[q(k-1)+\omega(k-1)]\end{aligned} \tag{16}$$

In general, we must compute the state transition matrix, Φ and input matrix, Γ using numerical integration and these matrices change from one time interval to the next. The solution to state Eq. (15) can be expressed as

$$X(t)=\Phi(t,t_0)X(t_0)+\int_{t_0}^{t}\Phi(t,\tau)[\Omega(\tau)q(\tau)+\Omega(\tau)\omega(\tau)]\,\mathrm{d}\tau$$

where state transition matrix $\Phi(t,\tau)$ is the solution to the following matrix homogeneous differential equation:

$$\dot{\Phi}(t,\tau)=\Psi(t)\Phi(t,\tau) \tag{17}$$

Next, we assume that $q(t)$ is a piecewise constant function of time for $t\in[t_{k-1},\,t_k]$ and set $t_0=t_{k-1}$ and $t=t_k$ in Eq. (17), to obtain

$$\Phi=e^{\Psi\Delta t}\simeq I+\Psi\Delta t$$

$$\Gamma=\int_{t_{k-1}}^{t_k}e^{\Psi(t_k-\tau)}\Omega\,\mathrm{d}\tau\simeq\Omega\Delta t+\Psi\Omega\frac{\Delta t^2}{2}\simeq\Omega\Delta t$$

X represent the state vector, Φ is the state transition matrix, Γ is the input matrix, q is the deterministic input sequence and $\omega(k-1)$ is a discrete-time white Gaussian sequence that is statistically equivalent through its first two moments to

$$\omega(k-1)=\int_{t_{k-1}}^{t_{k+1}}\Phi(t_k,\tau)\Omega(\tau)\omega(\tau)\,\mathrm{d}\tau$$

The mean and covariance matrix of $\omega(k-1)$ are

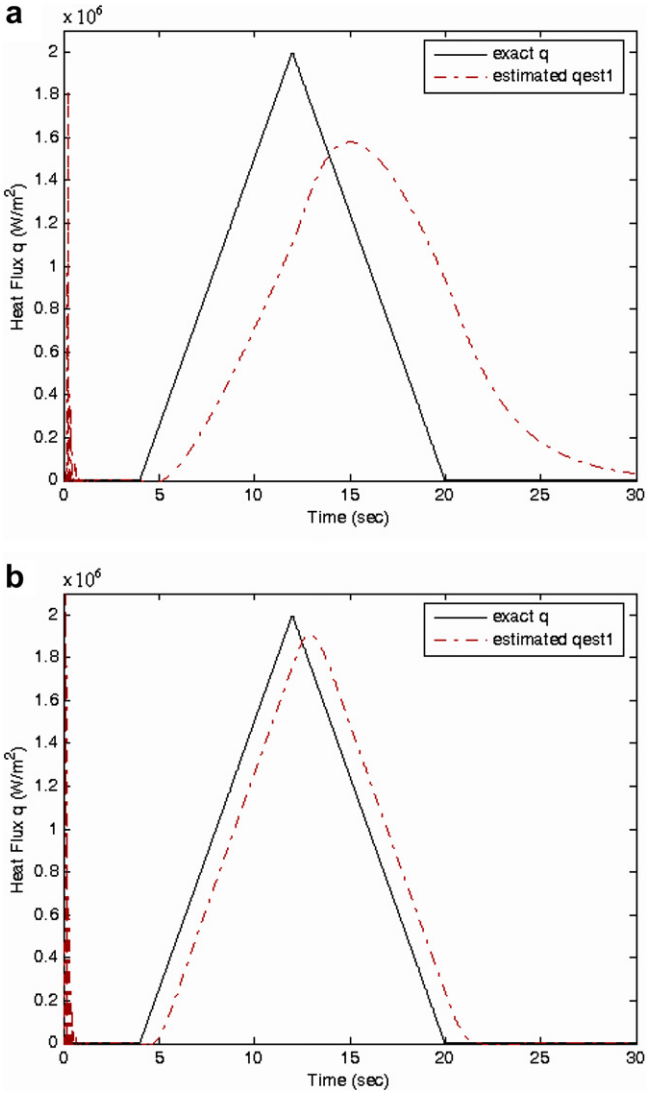

Fig. 3. Inverse estimation for $q(t)$ for Example 1 with $Q=10$, $N_{22}(0.11,0.08)$ ((a) $\sigma=0.001$ and (b) $\sigma=0.0001$).

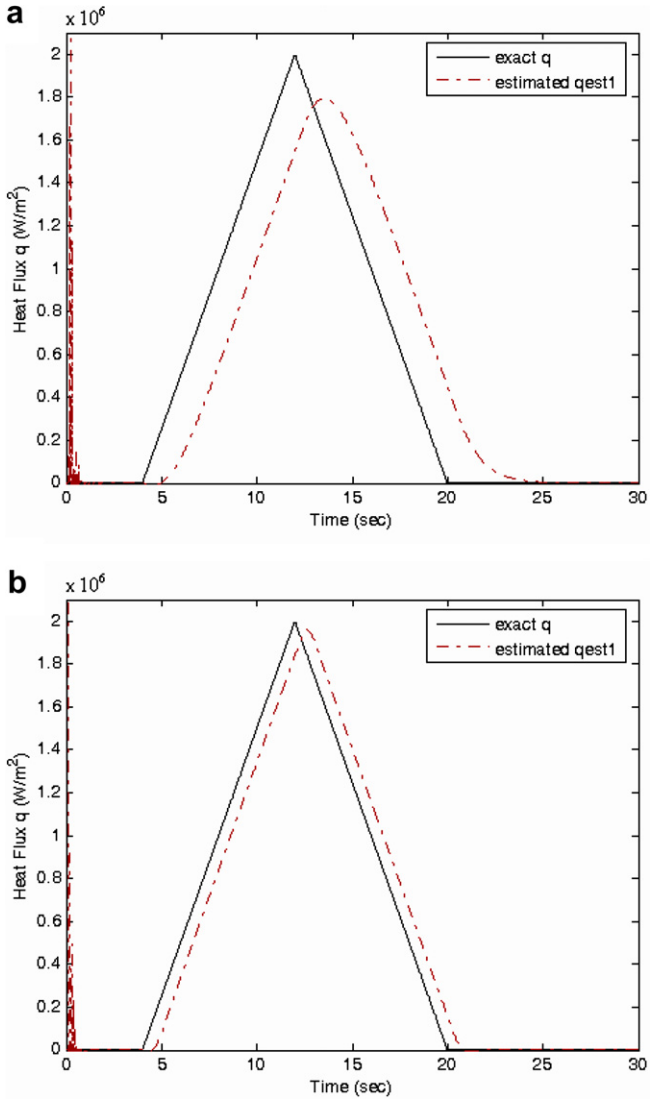

Fig. 4. Inverse estimation for $q(t)$ for Example 1 with $Q = 100$, $N_{22}(0.11, 0.08)$, ((a) $\sigma = 0.001$ and (b) $\sigma = 0.0001$).

$$E\{\omega(k-1)\} = E\left\{\int_{t_{k-1}}^{t_k} \Phi(t_k,\tau)\Omega(\tau)\omega(\tau)\,\mathrm{d}\tau\right\} = 0$$

$$E\{\omega(k)\omega^{\mathrm{T}}(j)\} = Q\delta_{kj} = Q \cdot I_{n\times n} \cdot \delta_{kj}$$

where $I_{n\times n}$ is the identity matrix. δ_{kj} is a Dirac delta function. Q is the covariance of processing error. Because our measurements have been assumed to be available only at sampled values of t at $t = t_i$, $i = 1, 2, \ldots$, In order to compare the results for situations involving measurement errors, we can express Eq. (7) as

$$Z(k) = HX_{\text{exact}}(k) + v(k) \tag{18}$$

Eqs. (16) and (18) constitute our discretized state-variable model. Where X_{exact} is the solution for the direct problem with a known $q(k)$, Z is the observation vector at time $k\Delta\tau$, H is the measurement matrix, v is the measurement noise vector, assumed to have zero mean and white noise. The variance of $v(k)$ is given by

$$E\{v(k)v^{\mathrm{T}}(j)\} = R\delta_{kj} = \sigma^2\delta_{kj}$$

where σ is the standard deviation of the measurement noise.

3. The adaptive weighting input estimation algorithm

The recursive input estimation algorithm consists of two parts. The first part is a Kalman filter. The second part is a real-time least squares algorithm. The input parameter is the unknown time-varying heat flux. The Kalman filter requires an exact knowledge of the process noise variance Q and the measurement noise variance R, R depends on the sensor measurements. The Kalman filter is used to generate the residual innovation sequence. This recursive real-time least-squares algorithm is derived by residual sequence to compute the value of the input heat flux. The actual values derived in the paper [20].

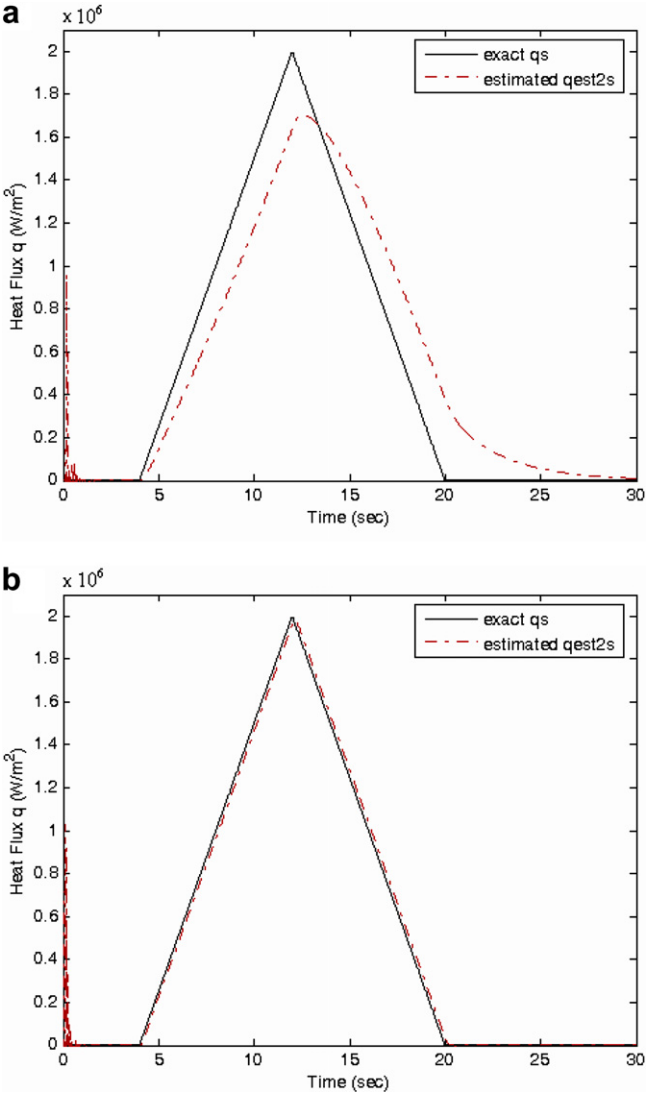

Fig. 5. Inverse estimation for $q(t)$ for Example 1 with $Q = 10$, $N_{45}(0.082, 0.018)$, ((a) $\sigma = 0.001$ and (b) $\sigma = 0.0001$).

The Kalman filter equations are given by

$$\overline{X}(k/k-1) = \Phi\overline{X}(k-1/k-1) \tag{19}$$

$$P(k/k-1) = \Phi P(k-1/k-1)\Phi^{\mathrm{T}} + \Gamma Q\Gamma^{\mathrm{T}} \tag{20}$$

$$s(k) = HP(k/k-1)H^{\mathrm{T}} + R \tag{21}$$

$$K(k) = P(k/k-1)H^{\mathrm{T}}s^{-1}(k) \tag{22}$$

$$P(k/k) = [I - K(k)H]P(k/k-1) \tag{23}$$

$$\overline{Z}(k) = Z(k) - H\overline{X}(k/k-1) \tag{24}$$

$$\overline{X}(k/k) = \overline{X}(k/k-1) + K(k)\overline{Z}(k) \tag{25}$$

The equations for a recursive least-squares algorithm are

$$B(k) = H[\Phi M(k-1) + I]\Gamma \tag{26}$$

$$M(k) = [I - K(k)H][\Phi M(k-1) + I] \tag{27}$$

$$K_b(k) = \gamma^{-1}P_b(k-1)B^{\mathrm{T}}(k) \times [B(k)\gamma^{-1}P_b(k-1)B^{\mathrm{T}}(k) + s(k)]^{-1} \tag{28}$$

$$P_b(k) = [I - K_b(k)B(k)]\gamma^{-1}P_b(k-1) \tag{29}$$

$$\hat{q}(k) = \hat{q}(k-1) + K_b(k)[\overline{Z}(k) - B(k)\hat{q}(k-1)] \tag{30}$$

where $\hat{q}(k)$ is the estimated input vector, $P_b(k)$ is the error covariance of the estimated input vector, $B(k)$ and $M(k)$ are the sensitivity matrices, and K_b is the Kalman gain. $\overline{Z}(k)$ is the bias innovation caused by measurement noise and input disturbance. $s(k)$ is the covariance of the residual. Here γ is an adaptive weighting function that may be presented as in [25]. That is

$$\gamma(k) = \begin{cases} 1 & |\overline{Z}(k)| \leqslant \sigma \\ \frac{\sigma}{|\overline{Z}(k)|} & |\overline{Z}(k)| > \sigma \end{cases} \tag{31}$$

using $\gamma(k)$ to replace the γ in Eqs. (28) and (29). When we let $\gamma = 1$, the above algorithm reduces to the usual sequential least-squares, which is suitable only for a constant–parameter system. The correction gain $K_b(k)$ for updating $\hat{q}(k)$, in Eq. (30), is diminishing as k increases, which allows $\hat{q}(k)$ to convergence to the true constant value. In the time-varying case, however, we like to prevent $K_b(k)$ from reducing to zero. This is accomplished by introducing the factor γ. For $0 < \gamma \leqslant 1$, $K_b(k)$ is effectively prevented from shrinking to zero. Hence, the corresponding algorithm can preserve its updating ability continuously. However, the inherent data truncation effect brought about γ causes variance increases $\hat{q}(k)$ in the estimation problem resulting from noise. Thus, it is necessary to compromise between fast adaptive capability and the estimate accuracy loss. A flow chart for the application of the recursive input estimation algorithm to the computation of $\hat{q}(k)$ is given in Fig. 2.

4. Results and discussion

To illustrate the accuracy of the proposed approach in predicting input heat flux $\hat{q}(k)$, the example is used to check the feasibility of the input estimation method including the finite-element scheme. The following physical quantities were used in the calculation:

Thermal properties of throat-insert material (polycrystalline graphite)	
Specific heat	$C_p = 1,046$ J/(kg °C)
Density	$\rho = 1,750$ kg/m^3
Thermal conductivity of axis	$K_{zz} = 120.9176$ J/(m s °C)
Thermal conductivity of radial	$K_{rr} = 69.036$ J/(m s °C)

The total time is t_f, the sampling interval $\Delta t = 0.005$ s and the unknown heat flux $q(z,t)$ is uniform applied to the inner counter surface. Thermocouples were placed in different nodes, respectively, elements number $E = 115$, total number of spatial nodes $N = 74$, the initial temperature $T_0 = 0$. $\gamma(k)$ is an adaptive weighting forget factor.

Where the error covariance of the estimated state is P, the error covariance of the estimated input vector is P_b. Because $P(-1/-1)$ and $P_b(-1)$ are normally unknown, the estimator was initialized with $P(-1/-1)$ and $P_b(-1)$ as very large numbers, such as 10^{10} and 10^{10}, respectively.

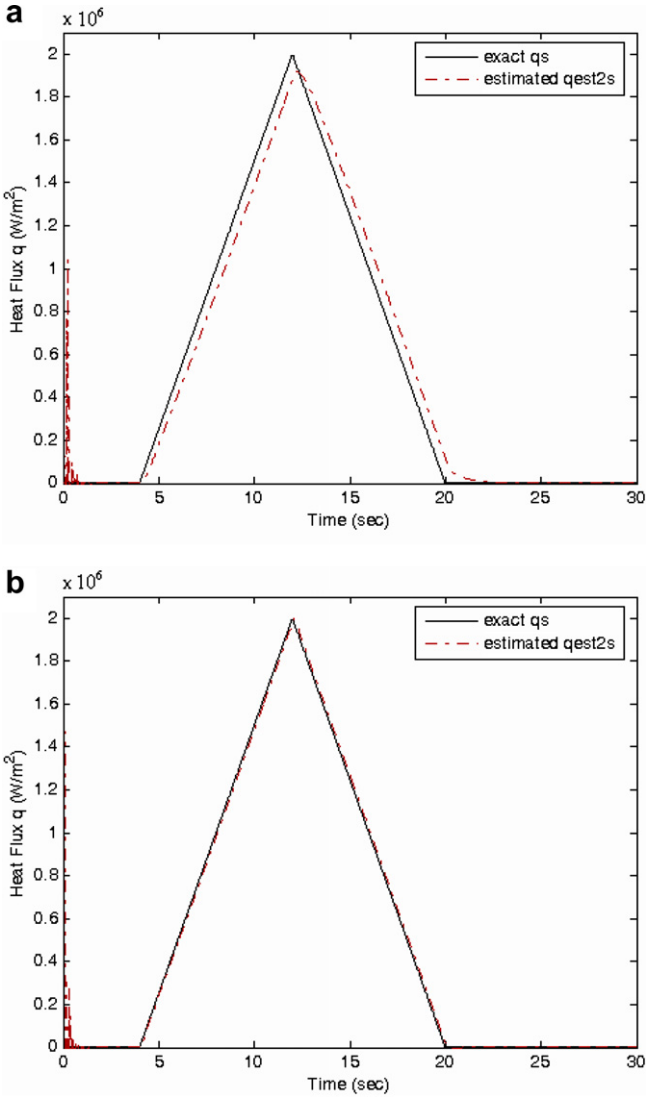

Fig. 6. Inverse estimation for $q(t)$ for Example 1 with $Q = 100$, $N_{45}(0.082, 0.018)$, ((a) $\sigma = 0.001$ and (b) $\sigma = 0.0001$).

This had the effect of treating the initial errors as very large. The estimator will therefore ignore the first few initial estimates [26]. The initial conditions for the input estimator were given by $\overline{X}(-1/-1) = [0 \quad 0 \quad \dots \quad 0]^{\mathrm{T}}$ and $P(-1/-1) = \mathrm{diag}[10^{10}]$ for the Kalman filter. The recursive least-squares algorithm initial conditions were given by $\hat{q}(-1) = [0 \quad 0 \quad 0 \quad \dots \quad 0]^{\mathrm{T}}$, $P_b(-1) = 10^{10} \cdot I_{n\times n}$ and $M(-1)$ was set using a zero matrix. The Kalman filter for the recursive input estimation algorithm requires exact knowledge of the process noise variance matrix Q and the measurement noise variance matrix R. R dependent on the sensor measurements. Both the value of Q in the filter and the value of $\gamma(k)$ in the sequential least-squares approach interactively affect the fast adaptive capability for tracking the time-varying parameter. The test input heat flux is given by

Example 1. Triangle waveform in $q(t)$ (W/m^2). The input heat flux $q(t)$ is assumed in the form

$$q(t) = \begin{cases} 0 & 0 \leqslant t < 4, 20 < t < t_f \\ 5\times 10^5 \times (0.5t - 2) & 4 \leqslant t \leqslant 12 \\ 5\times 10^5 \times (-0.5t + 10) & 12 \leqslant t \leqslant 20 \end{cases} \quad (\mathrm{W/m^2}) \tag{32}$$

First, we consider the estimation input heat flux $q(t)$ is triangle waveform on the inner counter surface, the outer wall surface are kept insulated, the sensors location are at $N_{22}(0.11, 0.08)$ and $N_{45}(0.082, 0.018)$, elements number $E = 115$, the initial temperature $T_0 = 0$, the sampling time interval $\Delta t = 0.005$ s, forgetting factor $\gamma(k)$, process noise covariance $Q = 10$, 100, and measurement noise covariance $\sigma = 0.001$, $\sigma = 0.0001$. The estimates of $q(t)$ are shown in Figs. 3–6. In this case, we use a triangle waveform heat flux

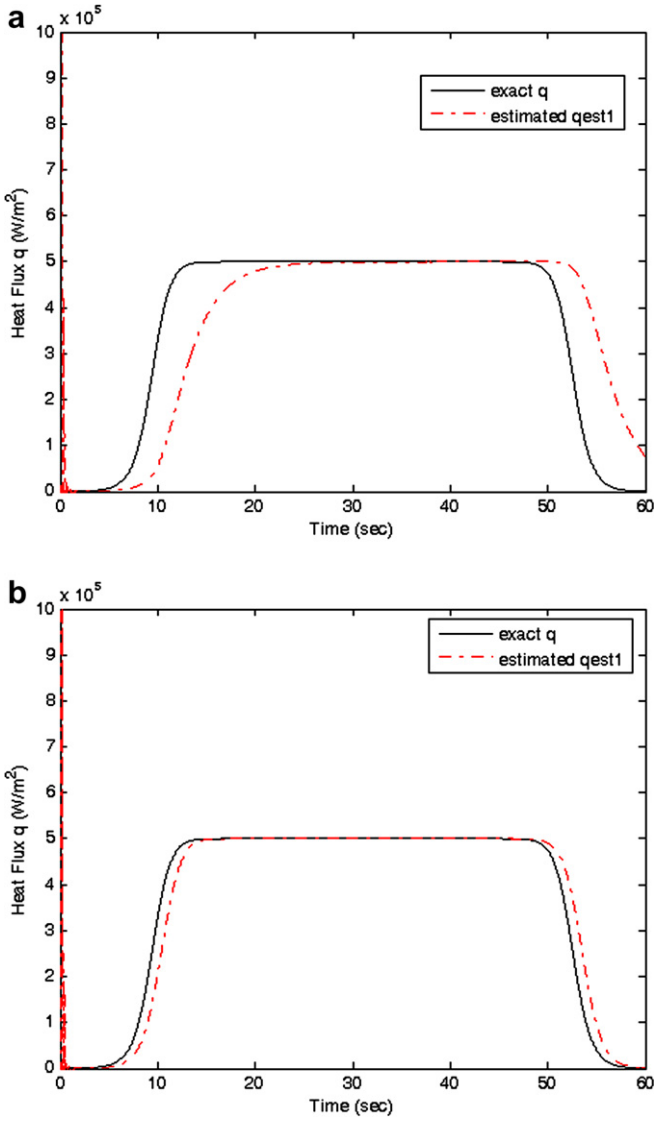

Fig. 7. Inverse estimation for $q(t)$ for Example 2 with $Q = 10$, $N_{22}(0.11, 0.08)$, ((a) $\sigma = 0.001$ and (b) $\sigma = 0.0001$).

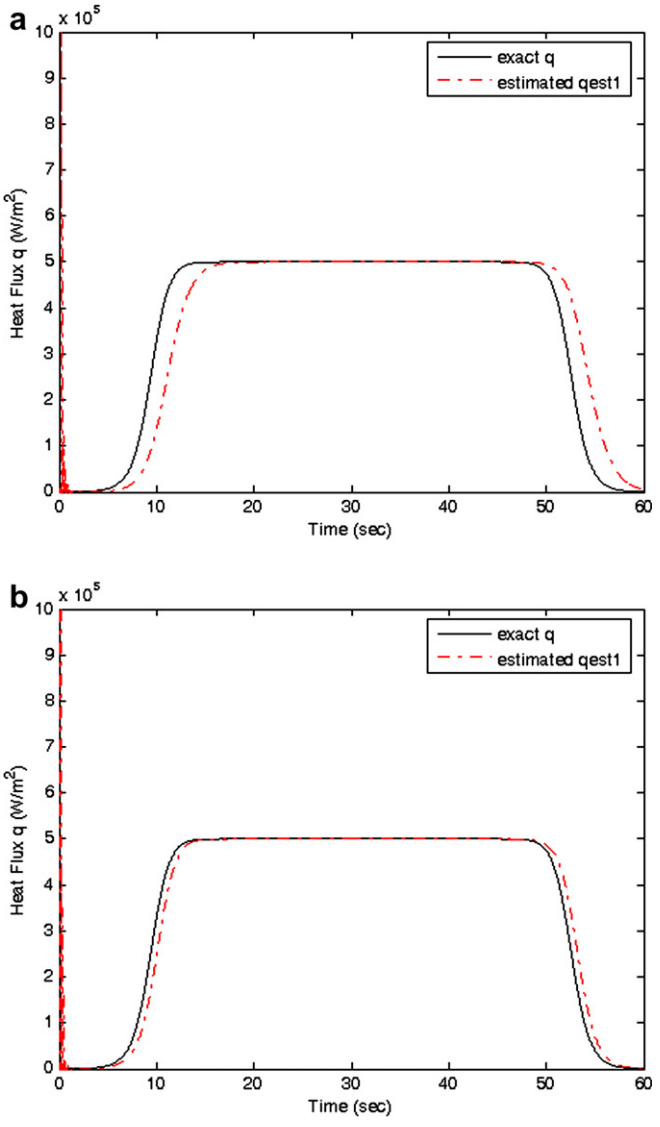

Fig. 8. Inverse estimation for $q(t)$ for Example 2 with $Q = 100$, $N_{22}(0.11, 0.08)$, ((a) $\sigma = 0.001$ and (b)$\sigma = 0.0001$).

to test this method. From Figs. 3–6, we find this method can estimate the unknown heat flux accuracy, and although the measurement error influences the estimate resolution, the results are still good.

Example 2. Generalized bell curve function waveform $q(t)$ (W/m^2) at the inner wall boundary. The input heat flux $q(t)$ is assumed in the form

$$q(t)=\begin{cases}0 & 0\leqslant t<1\\ 5\times 10^5\times\frac{1}{1+\left|\frac{(t-1)-c}{a}\right|^{2b}} & 1\leqslant t\leqslant t_f\\ a=21.6, b=11.5, c=30 & \end{cases}\quad (\mathrm{W/m^2}) \tag{33}$$

Here we consider the estimation input heat flux $q(t)$ is generalized bell curve function waveform on the boundary. It is in a manner like the missile flight with the high temperature jet flow which impact into the nozzle throat-insert inner contour during flight time. The following has assumption as mentioned above. The sensors location are at $N_{22}(0.11, 0.08)$ and $N_{45}(0.082, 0.018)$, elements number $E = 115$, the initial temperature $T_0 = 0$, the sampling time interval $\Delta t = 0.005$ s, forgetting factor $\gamma(k)$, process noise covariance $Q = 10$, 100, and measurement noise covariance $\sigma = 0.001$, $\sigma = 0.0001$. The estimates of $q(t)$ are shown in Figs. 7–10. Fig. 11 demonstrates the inner wall temperature figure.

From Figs. 7–11, just as the measurement variance R increases, the Kalman gain $K(k)$ Eq. (22) decreases. The correction Eq. (25) is proportional to the difference between that measurement and its best predicted value and when the σ increases, from Eq. (25) the Kalman gain $K(k)$ decrease causes the estimate more believe predicted value than new measurement. We can find that if the

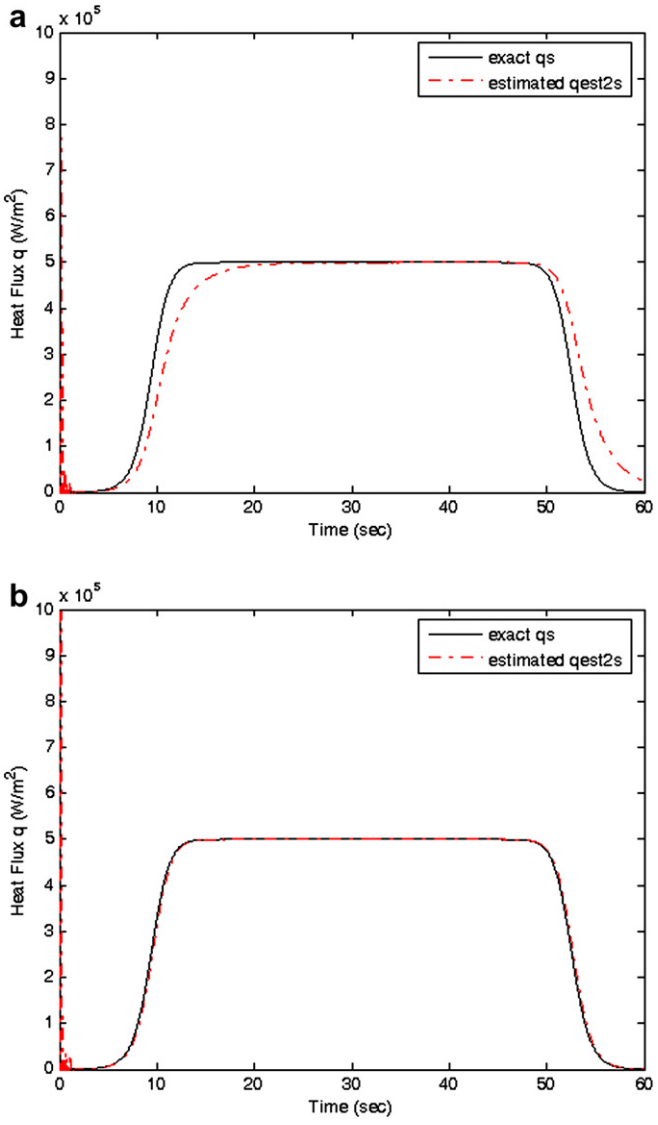

Fig. 9. Inverse estimation for $q(t)$ for Example 1 with $Q = 10$, $N_{45}(0.082, 0.018)$, ((a) $\sigma = 0.001$ and (b) $\sigma = 0.0001$).

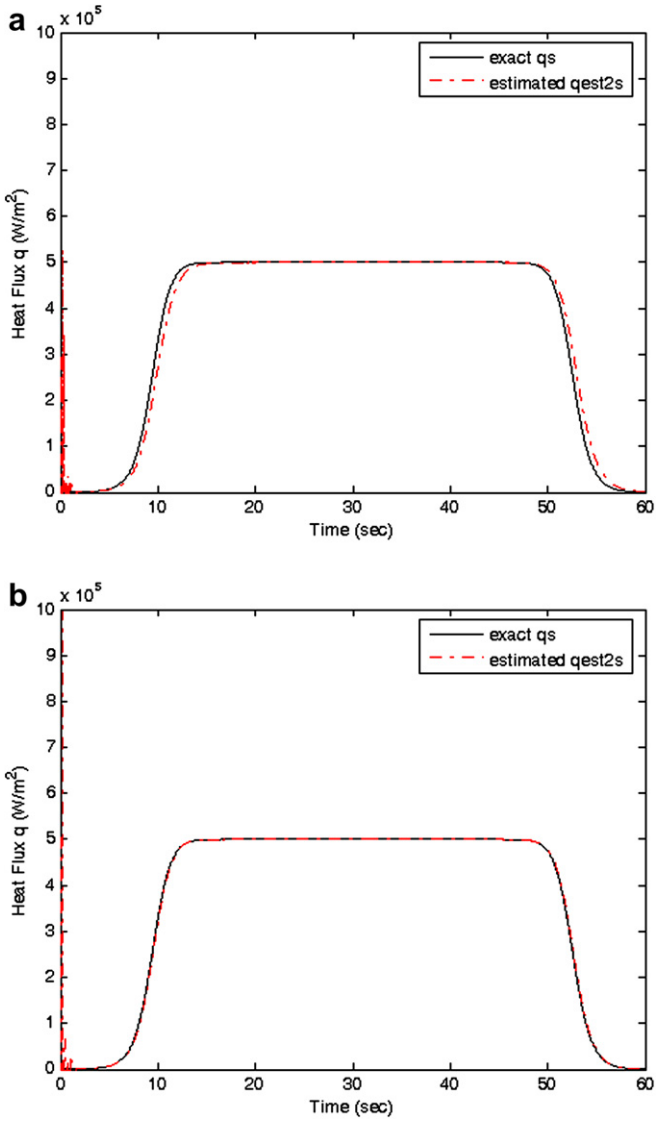

Fig. 10. Inverse estimation for $q(t)$ for Example 2 with $Q = 100$, $N_{45}(0.082, 0.018)$, ((a) $\sigma = 0.001$ and (b) $\sigma = 0.0001$).

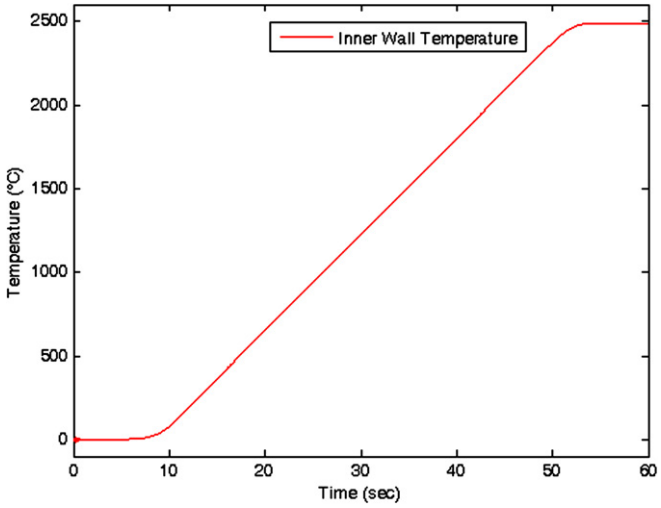

Fig. 11. Inner wall temperature.

modeling error (Q) from Eqs. (20)–(22) increases, it will make $K(k)$ increase, it leads to estimation quickly in Figs. 8 and 10. Figs. 7a, 8a, 9a and 10a show that a larger measurement error (σ) can cause estimation lag and estimate accuracy degradation, the results are still good. In Figs. 9 and 10, the sensor ($N_{45}(0.082, 0.018)$) approach the heat flux the lag effect smaller and the estimate result is better. The estimation results from the proposed method show excellent agreement with the exact value.

The above simulation results demonstrate that the proposed method has good performance in tracking unknown heat flux cases and the algorithm is capable of dealing with on-line 2D nozzle throat-insert inner contour irregular shape IHCP.

5. Conclusions

This research offered an effective analytical method for thermal-protection layer design in the solid rocket motor. We used simulations of the measured temperature on the nozzle throat-insert outer surface to estimate the heat flux in the inner wall on-line with accuracy. An on-line methodology, based on the input estimation method including the finite-element scheme, was developed for estimating unknown input heat flux on the boundary. A tradeoff between the process noise variance and sensitivity to measurement errors in inverse methods has been presented. We choose a larger model error ($Q = 100$) and precision measurement ($\sigma = 10^{-4}$) to acquire better estimated results. The polycrystalline graphite has been used for high pressure solid rocket motor nozzles working under extremely high heat flow and erosion. The result can use to internal insulation design of solid rocket motor. The proposed method is effective for IHCP. These applications can be useful in making quick and efficient identification of unknown heat flux on the inner surface, such as the heat source or heat flux of a thermal system. The method can be applied in certain types of problem and you can derive the state equation including unknown input, assuming the measurement equation is known. The unknown components at any time step can be estimated recursively from measurements taken at the same time step. In the future, it can be further applied to relative non-destruction tests. We will also expand this method to inverse heat conduction problems with irregular composite material geometries study or nonlinear system.

References

[1] W. Huazhen, Zhang Lei, W. Sun, Application of new ablatives in rocket nozzles, Acta Armament Arii 18 (3) (1997).
[2] P. Fu, Z. Jian, G. Zhang, B. Gao, Engineering calculation for erosion and thermal structure of throat-insert of a SRM nozzle, J. Solid Rocket Technol. 28 (1) (2005) 15–19.
[3] K. Zhang, Effect of ablation on nozzle inner contour on motor energy characteristics, J. Solid Rocket Technol. 20 (3) (1997) 26–28.
[4] C.H. Huang, M.N. Ozisik, Inverse problem of determining unknown wall heat flux in laminar flow through a parallel plate duct, Numer. Heat Transfer, Part A 21 (1992) 55–70.
[5] O.M. Alifanov, V.V. Millhailov, Solution of the nonlinear inverse thermal conducting problem by the iteration method, J. Eng. Phys. 35 (6) (1978) 1501–1506.
[6] V.V. Mikhailov, Questions of the convergence of iteration methods of solving the inverse heat conduction problem, J. Eng. Phys. 48 (1984) 1263–1265.
[7] E.P. Scott, J.V. Beck, Analysis of order of the sequential regularization solutions of inverse heat conduction problem, Trans. ASME 111 (1989) 218–224.
[8] C.H. Huang, Y.C. Wang, Inverse problem of controlling the interface velocity in Stefan problems by conjugate gradient method, J. Chinese Inst. Eng. 19 (2) (1996) 247–253.
[9] P.C. Tuan, L.W. Fong, W.T. Huang, Analysis of on-line inverse heat conduction problems, J. Chung Cheng Inst. Technol. 25 (1) (1996) 59–73.
[10] P.C. Tuan, L.W. Fong, W.T. Huang, Application of Kalman filtering with input estimation technique to on-line cylindrical inverse heat conduction problems, JSME Int. J., Series B 40 (1) (1997) 126–133.
[11] C.C. Ji, P.C. Tuan, H.Y. Jang, A recursive least-squares algorithm for on-line 1D inverse heat conduction estimation, Int. J. Heat Mass Transfer 40 (9) (1997) 2081–2096.
[12] C.C. Ji, H.Y. Jang, An inverse problem in predicting heat flux of M42 percussion primer, J. Franklin Inst. 335B (4) (1998) 595–604.
[13] N. Daouas, M.S. Radhouani, A new approach of the Kalman filter using future temperature measurements for nonlinear inverse heat conduction problems, Numer. Heat Transfer, Part B: Fundamentals 45 (6) (2004) 565–585.
[14] T.S. Prasanna Kumar, A serial solution for the 2D inverse heat conduction problem for estimating multiple heat flux components, Numer. Heat Transfer, Part B: Fundamentals 45 (6) (2004) 541–563.
[15] B.R. Bass, L.J. Ott, A finite element formulation of the two-dimensional inverse heat conduction problem, Adv. Comput. Technol. 2 (1980) 238–248.
[16] T. Yoshimura, K. Ituka, Inverse heat conduction problem by finite element formulation, Int. J. Syst. Sci. 16 (1985) 1365–1376.
[17] X. Ling, R.G. Keanini, H.P. Cherukuri, A non-iterative finite element method for inverse heat conduction problems, Int. J. Numer. Meth. Eng. 56 (9) (2003) 1315–1334.
[18] H.Y. Jang, P.C. Tuan, T.C. Chen, T.S. Chen, Input estimation method combined with the finite-element scheme to solve IHCP hollow-cylinder inverse heat conduction problems, Numer. Heat Transfer, Part A: Applications 50 (3) (2006) 263–280.
[19] T.C. Chen, P.C. Tuan, Input estimation method including finite-element scheme for solving inverse heat conduction problems, Numer. Heat Transfer, Part B: Fundamentals 47 (3) (2005) 277–290.

[20] P.C. Tuan, C.C. Ji, L.W. Fong, W.T. Huang, An input estimation approach to on-line two-dimensional inverse heat conduction problems, Numer. Heat Transfer, Part B 29 (1996) 345–363.
[21] J.F. Sun, B. Sun, S. Xiang, Theoretical calculation of complex nozzle's temperature profile and stress profile in solid rocket motor, J. Propulsion Technol. (1) (1994) 23–31.
[22] J.N. Reddy, Applied Functional Analysis and Variational in Engineering, Malabar, Florida, 1991.
[23] J.S. Larry, Applied Finite Element Analysis, East Lansing, Michigan, 1976.
[24] A.H. Jazwinski, Stochastic Processes and Filtering Theory, Academic Press, New York, 1970.
[25] P.C. Tuan, M.C. Ju, The validation of the robust input estimation approach to two-dimensional inverse heat conduction problems, Numer. Heat Transfer, Part B 37 (2) (2000) 247–265.
[26] Y.T. Chan, A.G. Hu, J.B. Plant, A Kalman filter based tracking scheme with input estimation, IEEE Trans. Aerospace Electron. Syst. AES-15 (1979) 237–244.